

# Ultraviolet nanophosphors

Bin Li<sup>a</sup>, Tom Hinklin<sup>b</sup>, Richard Laine<sup>b</sup>, Stephen Rand<sup>a,\*</sup>

<sup>a</sup>*Department of Electrical Engineering & Computer Science, USA*

<sup>b</sup>*Department of Materials Science, University of Michigan, Ann Arbor, MI, USA*

Available online 15 March 2006

## Abstract

Dopant-stabilized defect centers in alumina nanopowders are shown to be well-suited to efficient generation of ultraviolet cathodoluminescence.

© 2006 Elsevier B.V. All rights reserved.

*Keywords:* Rare earth oxides; Alumina; UV luminescence; Point defects

## 1. Introduction

Phosphors are widely available for display applications in the visible spectral region. This is the result of a century of active research on optical properties of semi conductors and dielectrics containing rare-earth impurities, transition metals, alkalis, and other dopants. Research on light emission in the range 250–290 nm on the other hand has been far more limited, because the radiation is invisible and very few solids either generate or transmit light efficiently at such short wavelengths, including scintillators.

The spectral range from 250–290 nm overlaps key protein absorption bands. So efficient UV phosphors in this range can be useful for decontamination and medical applications. Protein and DNA absorption bands in the ultraviolet extend from 250 to 290 nm. Radiation in this range causes damage to amino acid linkages and when combined with X-ray radiation can effectively decontaminate/sterilize contaminated surfaces. Sources in this range are also potentially important for replacing Hg discharge sources in water purification systems.

There are only a few reasonable candidates for ultraviolet-emitting solids that could replace Hg sources for applications requiring high flux. Here we consider rare-

earth-doped solids, wide band gap semiconductors, and point defects.

## 2. Experimental methods

Flame spray pyrolysis (FSP) was used to prepare two kinds of sample for this study [1]. The first was  $\delta$ -Al<sub>2</sub>O<sub>3</sub> doped with 1000 ppm Ce<sup>3+</sup>. The second was  $\delta$ -Al<sub>2</sub>O<sub>3</sub> doped with MgO to provide twenty concentrations between 0.2 and 50 mol%.

The composition and phase of these samples were determined using X-ray diffraction (XRD) and as-grown powders mounted in ultrahigh vacuum for electron beam irradiation and cathodoluminescence studies. Representative XRD traces are given in Fig. 1, to illustrate the production of different phases by FSP through variation of the Mg concentration in the Mg-doped series. The X-ray curves illustrate the significant degree of phase control that is possible through synthesis of oxide nanopowders by flame spray pyrolysis. At low Mg concentration the indexed patterns revealed a mixture of orthorhombic, tetragonal and monoclinic phases. At intermediate Mg concentration, the nanopowders were predominantly of the tetragonal phase. At high concentration only MgAl<sub>2</sub>O<sub>4</sub> (spinel) was found.

As-grown samples were loaded into an ultrahigh vacuum chamber and subjected to a 6 keV electron beam at currents ranging from 5 to 50  $\mu$ A in a 1 mm spot.

\*Corresponding author. Tel.: +1 734 763 6810; fax: +1 734 647 2718.  
E-mail address: [scr@umich.edu](mailto:scr@umich.edu) (S. Rand).

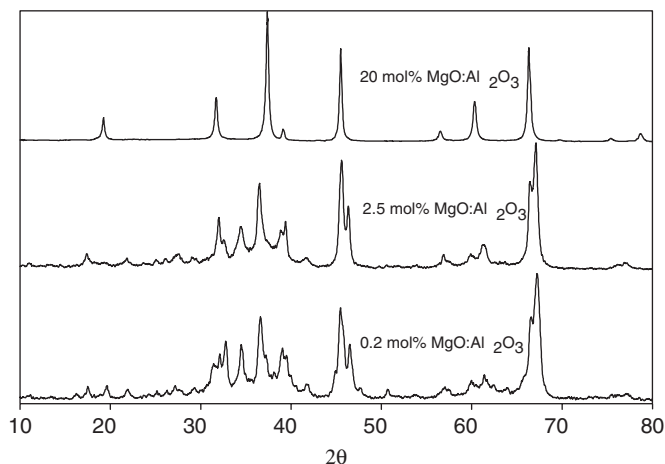


Fig. 1. X-ray diffraction patterns of selected LF-FSP MgO:Al<sub>2</sub>O<sub>3</sub> powders. The 0.2 mol% MgO sample is a mixture of orthorhombic, tetragonal and monoclinic phases. The 2.5 mol% MgO sample is nearly pure tetragonal. The 20 mol% MgO sample is purely cubic spinel.

Cathodoluminescence was collected and analyzed with 0.25 and 1.0 m grating spectrometers using a photomultiplier and photon counting electronics.

### 3. Results

#### 3.1. Rare-earth-doped phosphors

Trivalent rare-earth ions have relatively low oscillator strengths on 4f–4f transitions because these transitions are forbidden by Laporte's rule. Consequently, unless stimulated emission can be achieved in the phosphor material, ions like Nd<sup>3+</sup> whose high-lying <sup>2</sup>F levels have a ground state transition near 260 nm are not useful for decontamination applications. Inter-configurational transitions on the other hand (for example 5d–4f transitions) are fully allowed. Emission from Ce<sup>3+</sup>-doped solids on the allowed 5d–4f transition is potentially useful for this reason.

Stimulated emission can be obtained from inverted Ce ions on the ultraviolet 5d–4f transition in very fine powders pumped by an electron beam. The way in which multiple scattering mediates this process has been discussed previously [2]. In this work the potential importance of Cerium for solid state ultraviolet emission sources was confirmed by new experiments and reconsidered for this high flux application. Unfortunately, the Cerium emission spectrum does not extend below 310 nm in alumina, and not below 280 nm in fluoride hosts [3]. So while it was confirmed to provide efficient ultraviolet “laser phosphor” operation close to the protein absorption band, it must be concluded that Ce<sup>3+</sup>-doped oxide phosphors per se are unsuitable for operation at 265 nm.

#### 3.2. Wide band gap semiconductors

Wide band gap ternary alloys like Al<sub>x</sub>Ga<sub>1-x</sub>N offer additional possibilities for UV source technology in the

range 240–280 nm. While emission properties of Al<sub>x</sub>Ga<sub>1-x</sub>N are not reported here, the band gap of this material can clearly be adjusted with appropriate compositions to yield band-to-band emission at 265 nm. Unfortunately surface states often lead to undesired absorption in powdered semiconductors, and this generally necessitates the use of high-quality growth techniques and passivation of particle surfaces. While Al<sub>x</sub>Ga<sub>1-x</sub>N thin films prepared by molecular beam epitaxy (MBE) or chemical vapor deposition (CVD) have high quantum efficiency, these approaches are relatively expensive. There are currently no high yield methods available for the production of Al<sub>x</sub>Ga<sub>1-x</sub>N phosphors with high radiant efficiency. Direct deposition of thin Al<sub>x</sub>Ga<sub>1-x</sub>N films on suitable electrode structures may nevertheless furnish high brightness and efficient emission at 265 nm. Even polycrystalline films might support random laser action similar to previous results in ZnO films [4].

#### 3.3. Point defect centers

Of main interest in this paper for short wavelength generation are point defects created in FSP powders during the rapid thermal quench step following combustive synthesis (Figs. 2 and 3). In the spectra to follow, these consist of single oxygen vacancies and their aggregates, in various states of ionization and association with divalent Mg impurities. Single electrons occupying anion vacancies in crystalline solids have intrinsically high quantum efficiencies [5]. Even two-electron centers have quantum efficiencies approaching unity when inter-system crossing is avoided. For example the F<sup>+</sup> center in MgO has an oscillator strength of 0.8 [6] and the F<sup>+</sup> center in Al<sub>2</sub>O<sub>3</sub> has a decay time of 50 ns at a wavelength of 325 nm [7], indicating a similar high radiative efficiency.

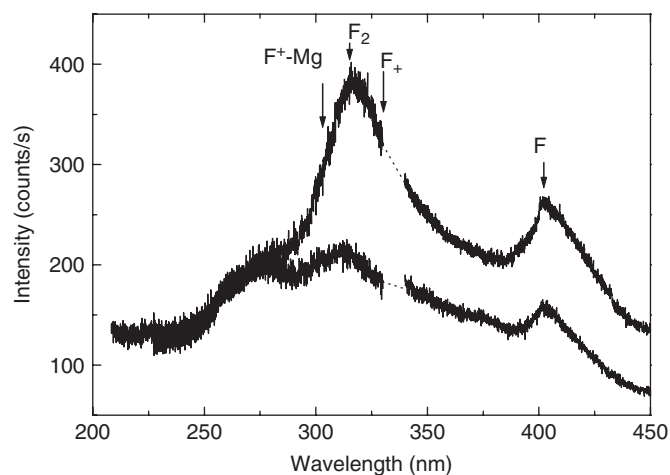


Fig. 2. Ultraviolet cathodoluminescence from 2.5% Mg-doped Al<sub>2</sub>O<sub>3</sub> nanopowder. Acceleration voltage was 6 kV. The two traces correspond to beam currents of 10 (upper) and 30 (lower) microamps and reveal dramatic changes in the relative concentration of F-centers at room temperature. The spectral gap near 330 nm resulted from changing spectral orders to cover the range 200–450 with the 1 m grating spectrometer.

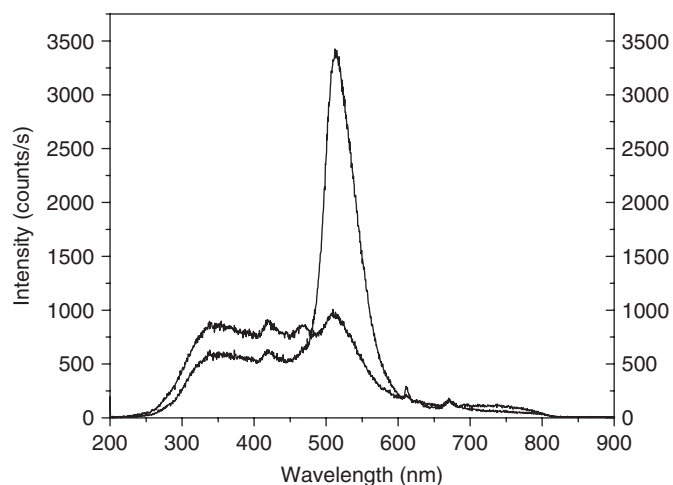


Fig. 3. Cathodoluminescence of 20%Mg:Al<sub>2</sub>O<sub>3</sub> nanopowders at 6kV. Two curves are shown, one at 10 (upper trace at 520nm) and one at 30 (lower trace at 520nm) microamps. Data was acquired with a 0.25m grating spectrometer. Resolution was 1 nm.

Table 1  
Absorption and emission of point defects in sapphire (references are given in parentheses)

Material	Defect	Abs. peak (nm)	Em. peak (nm)
Al <sub>2</sub> O <sub>3</sub>	F	205	420 [7]
Mg:Al <sub>2</sub> O <sub>3</sub>	F <sup>+</sup> -Mg	255	310 [8]
Al <sub>2</sub> O <sub>3</sub>	F <sup>+</sup>	258	325 [7]
Al <sub>2</sub> O <sub>3</sub>	F <sub>2</sub>	300	322 [7]
Al <sub>2</sub> O <sub>3</sub>	F <sub>2</sub> <sup>+</sup>	355	379 [7]
Al <sub>2</sub> O <sub>3</sub>	F <sub>2</sub> <sup>2+</sup>	455	550 [7]

In Mg-doped sapphire, the presence of Mg on a site neighboring an F<sup>+</sup> center shifts the emission wavelength to a shorter value [8]. Since divalent cations can stabilize and shorten the emission wavelength of ionized F-centers, mixed oxides of MgO and Al<sub>2</sub>O<sub>3</sub> are intriguing candidates for UV generation. Some of the basic characteristics of the primary F-centers in alumina are listed in Table 1. F<sup>+</sup>-centers with Mg<sup>2+</sup> substituting for Al<sup>3+</sup> on neighboring sites (designated as F<sup>+</sup>-Mg centers in this paper) also give rise to even shorter wavelength emission that arises from recombination of holes with F<sup>+</sup>-Mg centers. F<sup>+</sup>-Mg centers have a high cross section for hole recombination, higher in fact than that of isolated F<sup>+</sup>-centers [8]. Recombination of ionized oxygen vacancy centers therefore decreases the density of F<sup>+</sup>-Mg and F<sup>+</sup>-centers during electron irradiation. Taken together with changes in the number of electrons residing in aggregate F-centers (like the divacancy center F<sub>2</sub>), this accounts for the reduced emission intensity of many spectral features at high currents (Figs. 2 and 3).

For reasons not entirely understood, there is an ultraviolet emission band between 250 and 290 nm that shows anomalous “bleaching” behavior. At 20 mol% Mg concentration the intensity of this band is higher at 30 μA

than it is at 10 μA (Fig. 3). At 2.5 mol% Mg concentration the intensity of this band is slightly lower at 30 μA than that at 10 μA. At 0.2 mol% Mg concentration the intensity of this band is once again considerably higher at 30 μA than it is at 10 μA. Hence the capability of generating light in the short wavelength band at high current levels improves as the Mg concentration is increased. At the highest Mg concentrations, spectral features in the range 300–500 nm also appear to be stabilized, although the large F<sub>2</sub> emission peak seen at low current near 520 nm clearly exhibits a strong bleaching effect similar to the reduction of emission seen in Fig. 2 at elevated current levels. The spectrum of the 20% sample does not extend far into the visible and near infrared. A greater proportion of the emission emerges in the ultraviolet and was most intense at the highest doping level synthesized, namely 50%Mg.

#### 4. Conclusions

Optical measurements with over twenty different Mg concentrations have shown that pyrolytic synthesis can produce high densities of point defects in alumina. This unusual finding is a by-product of kinetic synthesis. Mg:Al<sub>2</sub>O<sub>3</sub> has good potential for ultraviolet emission in the range 250–290 nm. Emission intensities in this spectral range show systematic variations that reflect changes in the crystal phases of alumina as well as variations in Mg concentration. The stability of ultraviolet emission features in the range 250–290 nm is best in alumina samples with high Mg concentrations (>20%).

While no results have been published as yet on stimulated emission of color centers in alumina nanopowders, preliminary results in our laboratory indicate that just as in Ce-doped samples, random lasing can be achieved with point defects in oxide powders. Hence the combination of an enhanced stimulated emission rate with the natural characteristics of F<sup>+</sup>-Mg defect emission may provide superior performance in the future. Ce-doped fluorides (Ce:LiSrAlF<sub>6</sub> and CeF<sub>3</sub>) and nitride semiconductors may also provide useful sources.

#### References

- [1] R.M. Laine, T. Hinklin, G. Williams, S.C. Rand, J. Metastable Nanocryst. Mater. 8 (2000) 500.
- [2] G.R. Williams, B. Bayram, S.C. Rand, T. Hinklin, R.M. Laine, Phys. Rev. A 65 (2001) 013807.
- [3] V.V. Semashko, M.A. Dubinskii, R.Y. Abdulsabirov, A.K. Naumov, S.L. Korableva, N.K. Scherbakova, A.E. Klimovitskii, Laser Phys. 5 (1) (1995) 69.
- [4] H. Cao, Y.G. Zhao, S.T. Ho, E.W. Seelig, Q.H. Wang, R.P.H. Chang, Phys. Rev. Lett. 82 (1999) 2278.
- [5] W.B. Fowler, Physics of Color Centers, Academic Press, New York, 1968.
- [6] B. Henderson, R.D. King, Philos. Mag. 13 (1966) 1149.
- [7] Y. Chen, M.M. Abraham, Nucl. Instrum. Methods B 59–60 (1991) 1163.
- [8] P.A. Kulis, M.J. Springis, I.A. Tale, V.S. Vainer, J.A. Valbis, Phys. Status Solidi. B 104 (1981) 719.